

INTRODUCTION

Nuclear waste disposal requires the establishment of numerous barriers between the waste and man's environment such that a large safety margin exists with very low probability of complete barrier failure. Deep burial provides a natural geologic barrier. However, the prediction of the nuclide retardation provided by the geologic barrier requires knowledge of the hydrological and chemical properties of the formation.

Volcanic tuff at the Nevada Test Site (NTS) is being evaluated as a potential waste disposal medium. A field nuclide migration experiment has been proposed in order to evaluate hydrologic properties, examine chemical reactions with tuff, and verify current numerical transport models (Erdal, et al, 1981). Because of the potential for groundwater to transport radionuclides in the jointed tuff, the focus of the project has been on understanding flow in a single fracture.

The hydrology of fractured rock is in the early stages of development; hence, there are few large-scale laboratory or field experiments to emulate. The nuclide experiment as presently conceived, involves drilling instrumentation holes with axes parallel to the joint plane. However, the drill holes alter the normal stress at the joint which changes the joint aperture and significantly affects the joint permeability. Hence, comparisons of field results with numerical models are made more difficult.

A dominating feature of the flow behavior is the fracture permeability. This report attempts to evaluate effects of the present experiment configuration on the fracture permeability.

*ROCK discontinuities or failure surfaces are often referred to as: 1) faults when lateral movement has occurred along the failure plane, 2) joints when subparallel sets of failure surfaces exist, and 3) fissures for discontinuities which are small in extent and aperture. The term fracture is usually a more general description of a failure surface. However, for this report fracture and joint are used interchangeably to describe a single failure surface.

ANALYSIS

Stresses

In rock stressed below one-half its ultimate compressive strength and in which joints are tight and widely spaced, it is usually acceptable to consider the rock as a continuous, linearly elastic material (Goodman, 1980). By also assuming the rock is homogeneous, isotropic, and isothermal, the stress distribution around a cylindrical hole is described by the Kirsch solution (Poulos and Davis, 1974). (Terms are defined in Figure 1.)

$$\frac{\sigma_r}{\sigma_y} = \frac{1+n}{2} \left[1 - \left(\frac{a}{r}\right)^2 \right] + \frac{1-n}{2} \left[1 - 4\left(\frac{a}{r}\right)^2 + 3\left(\frac{a}{r}\right)^4 \right] \cos 2\theta$$

$$\frac{\sigma_\theta}{\sigma_y} = \frac{1+n}{2} \left[1 + \left(\frac{a}{r}\right)^2 \right] - \frac{1-n}{2} \left[1 + 3\left(\frac{a}{r}\right)^4 \right] \cos 2\theta$$

$$\frac{\tau_{r\theta}}{\sigma_y} = -\frac{1-n}{2} \left[1 - 3\left(\frac{a}{r}\right)^4 + 2\left(\frac{a}{r}\right)^2 \right] \sin 2\theta$$

The above formulation does not include gravity forces (and thus there is no size effect) since gravity forces on the small drill holes proposed would be negligible.

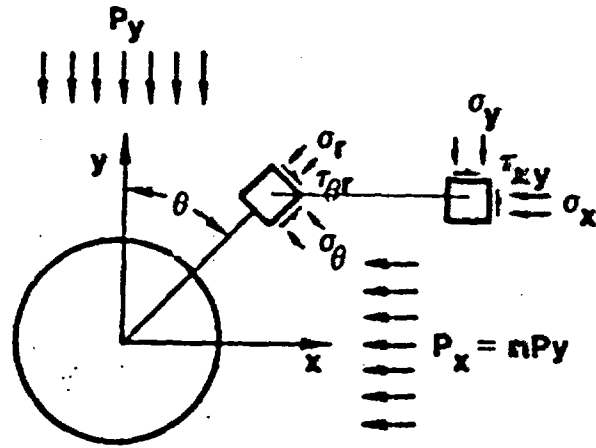
Determining the stresses in the x and y directions by the following familiar equations:

$$\sigma_x = \frac{\sigma_\theta + \sigma_r}{2} + \left(\frac{\sigma_\theta - \sigma_r}{2} \right) \cos 2\theta + \tau_{r\theta} \sin 2\theta$$

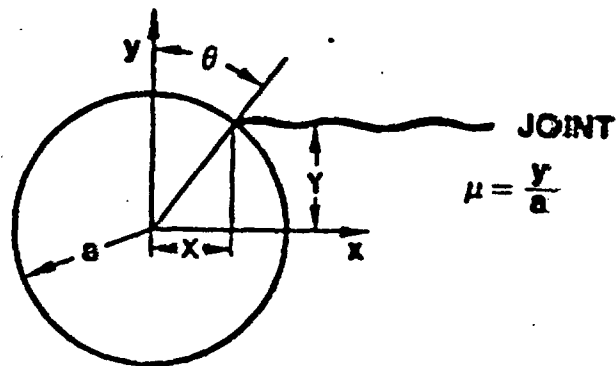
$$\sigma_y = \frac{\sigma_\theta + \sigma_r}{2} - \left(\frac{\sigma_\theta - \sigma_r}{2} \right) \cos 2\theta - \tau_{r\theta} \sin 2\theta$$

$$\tau_{xy} = - \left(\frac{\sigma_\theta - \sigma_r}{2} \right) \sin 2\theta + \tau_{r\theta} \cos 2\theta$$

DEFINITION OF TERMS



(a)



(b)

Figure 1. Definition of Terms: a) Cylindrical Drill Hole in Solid Mass Under Plane Strain, Isothermal, and Elastic Conditions; b) Drill Hole - Fracture Configuration

and expressing the results in normalized, Cartesian coordinates, one obtains:

$$\frac{\sigma_y}{P_y} = \left[s - 2t \frac{b}{a^2} \right] - \frac{b}{a^2} \left[s - tb \left(1 - \frac{2}{a} + \frac{3}{a^2} \right) \right] + 4t \left(\frac{u\lambda}{a} \right)^2 \left(1 + \frac{2}{a} - \frac{3}{a^2} \right) \quad (1)$$

$$\frac{\tau_{xy}}{P_y} = \frac{2u\lambda}{a^2} \left[2t \frac{b}{a} \left(\frac{3}{a} - 2 \right) - s \right] \quad (2)$$

where

$$a = \frac{x}{a}$$

$$b = u^2 - a^2$$

$$u = \frac{y}{a}$$

$$s = \frac{1+n}{2}$$

$$a = u^2 + a^2 = \frac{1}{a^2} (y^2 + x^2)$$

$$t = \frac{1-n}{2}$$

Equations (1) and (2) describe the stress field around a drill hole in a continuum. If it is assumed a joint does not induce stress changes, stresses along a hypothetical joint can be calculated. Figure 2 plots equation (1) for three horizontal-vertical stress ratios: $P_x = nP_y$, $n = 0.5$, $n = 1.0$, and $n = 2.0$. The curves terminate at the point of intersection of the fracture with the drill hole. Both Figures 2a and 2b (horizontal stress less than or equal to the vertical stress) are similar in shape. In both cases the normal stress increases dramatically as the joint plane approaches the drill hole axis ($u = Y/a = 0.0$).

When the horizontal stress is twice as large as the vertical stress ($n = 2.0$), the stress change due to the drill hole does not show a uniform progression. This phenomenon causes odd behavior in the permeability changes as seen in Figure 4 which is discussed later. (This stress condition

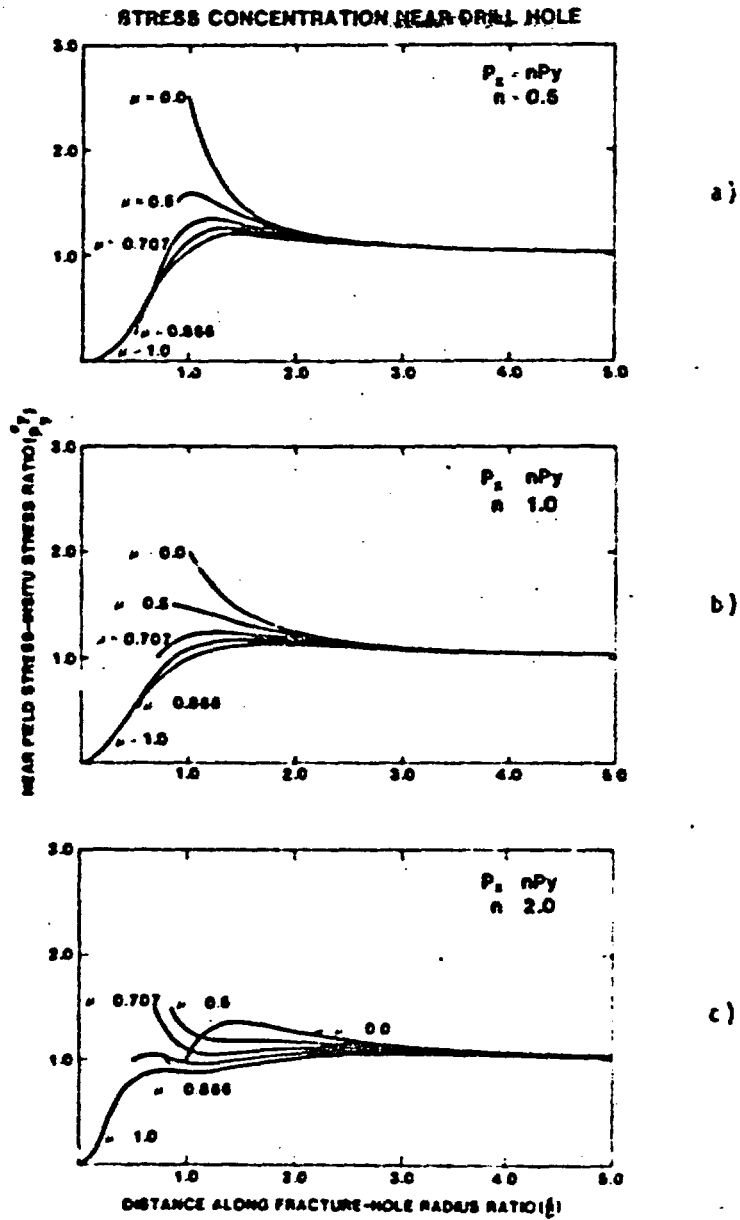


Figure 2. Normal Stress Concentration Along a Joint for Three Horizontal-Vertical Stress Ratios, $P_x = nP_y$
 a) $n = 0.5$ b) $n = 1.0$ c) $n = 2.0$.

exists at several places where the nuclide migration experiment may be conducted.) It is evident, however, that the normal stress excursion decreases for all μ as n increases in regions beyond the circle radius ($x/a > 1$).

The optimal drill hole position is that which minimizes stress changes. A tangential intersection of the drill hole clearly minimizes the joint normal stress changes for $n \leq 1$. As n increased beyond 1.0, the optimal position shifts to $\mu = 0.866$. A tangential intersection only slightly relieves joint stresses. However, it is still nearly optimal.

For a tangential intersection, unusual stress behavior might occur in the small triangular region between $0 < x/a < 1$. It is likely the joint would open slightly. It is also possible for the triangular region to break out during drilling. However, it was assumed the joint did not introduce any change in the stress field. The validity of this continuum approach was verified by evaluating shear stresses along the joint and comparing with shear strength for possible slippage. Figure 3 plots the ratio of the shear stress and the near field, normal stress (τ_{xy}/σ_y) versus x/a . The relationship was obtained from equations (1) and (2).

Goodman (1976) states that generally the coefficient of friction ($f = \tau/\sigma_n$ where τ = shear stress and σ_n = normal stress) varies in the range of 0.4 to 0.8 and can drop as low as 0.2 for sheet minerals such as mica. Byerlee (1978) found that at intermediate normal stress (1-150 ksi or 5-100 MPa) the friction generated was independent of rock type and initial surface roughness and equal to about 0.85. The latter friction coefficient value was plotted on Figure 3.

It is seen that only a small segment of the joint is subjected to shear stresses great enough to cause slippage. No slippage is predicted for x/a values greater than 1.06. When the horizontal stress is equal to or less than the vertical stress no slippage is predicted beyond $x/a = 0.82$. Thus it appears reasonable to model the rock mass as a continuum without a joint for points beyond the hole radius.

Permeability

Fracture permeability (k) is a function of confining pressure (P_c), internal fluid pressure (P_f), temperature, aperture (e) and surface roughness (Kranz, et al, 1979). Analytically, the fracture permeability is frequently related to the square of the aperture (e) from a parallel plate model (Bear, 1972). (The aperture, in turn, is dependent on the loading due to present and past mechanical, thermal, and fluid stresses.)

$$k = \frac{e^2}{12}$$

or

$$Q/\Delta h \propto ke = \frac{e^3}{12} \quad (\text{cubic law}) \quad (3)$$

where

k = fracture intrinsic permeability = $(n/\gamma)K$ (L^2)

K = hydraulic conductivity (L/T)

n = viscosity (M/LT)

γ = specific weight (M/L^2T^2)

e = crack aperture (L)

Q = discharge (L^3/T)

h = hydraulic head change (L)

Witherspoon, et al, (1980) found the cubic law to uniquely define permeability whether the fractures were held open or closed under stress. More importantly the results were independent of rock type, loading path, and load history.

It is readily apparent that while permeability might be uniquely determined by aperture, fracture dimensions cannot be determined in the field. Thus, the relationship of aperture or permeability versus applied stress must be known. Unfortunately, permeability and aperture do not appear to be unique functions of stress. Several experimenters (Kranz, et al, 1979; Iwai, 1976; Nelson and Handin, 1977) have found permanent alterations

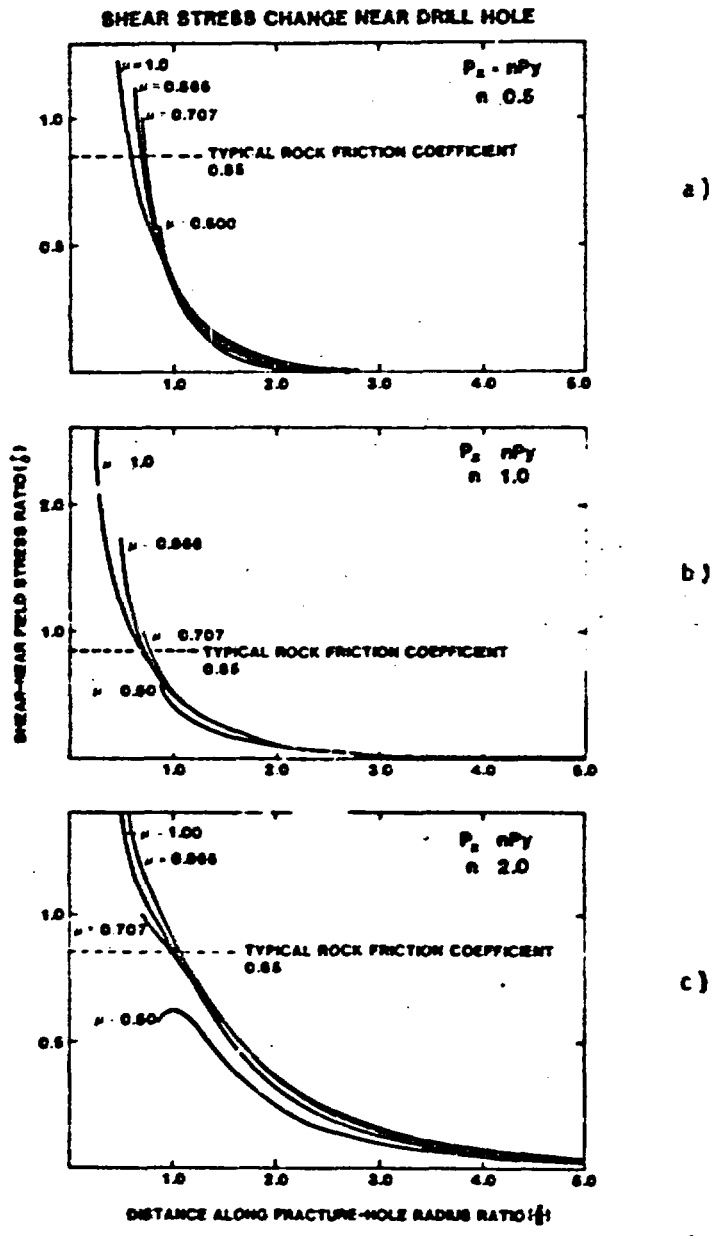


Figure 3. Shear Stress Changes Along a Joint for Three Horizontal-Vertical Stress Ratios, $P_x = nP_y$
 a) $n = 0.5$ b) $n = 1.0$ c) $n = 2.0$.

(hysteresis) of permeability under cyclic loading. However, after 4 to 5 cyclic loadings at similar stress levels, repeatable permeability-stress curves were often produced (Iwai, 1976). This observation is similar to the situation encountered in soil consolidation tests.

Gangi (1978) has published a power-law permeability-stress relationship using a bed-of-nails model as follows:

$$\left(\frac{k_e}{k_e'}\right)^{1/3} = 1 - \left(\frac{P_f}{E}\right)^m$$

where

- k_e' = zero pressure permeability-aperture product (L^3)
- E = effective modulus of asperities (M/LT^2)
- P_f = fluid pressure (M/LT^2)
- m = constant characterizing distribution function of asperity lengths, $0 < m < 1$ (m would supposedly change after each loading)

For this study, stress effects on the joint aperture were evaluated by using the preliminary results obtained by Walsh (1981):

$$\left(\frac{k_e}{k_0 e_0}\right)^{1/3} = \left(1 - \frac{\sqrt{2}b}{e_0}\right) \ln\left(\frac{P}{P_0}\right)_e \quad (4)$$

where

- $k_0 e_0$ = permeability-aperture product at reference state (L^3)
- $(P/P_0)_e$ = ratio between unknown and reference effective pressures
- b = r.m.s. of fracture surface protuberances (L)

Equation (4) is similar in form to Jones' (1975) empirically derived formula: $(k_e)^{1/3} = A - B \ln P_c$ where P_c denotes the confining pressure. Both Walsh (1981) and Gangi (1978) have applied their equations to carbonate rock data collected by Jones (1975) and found fairly good agreement.

By assuming the validity of equation (3), it is possible to derive an expression for the aperture (e) using equation (4):

$$e = e_0 \left[1 - \frac{\sqrt{2} b}{e_0} \ln \left(\frac{P}{P_0} \right) \right]$$

The parameter b would presumably account for hysteresis effects as stress was applied and taller asperities crushed.

From data found in Kranz, et al (1979) and Barre and Stesky (1980), Walsh back-calculated the term $\sqrt{2} b/e_0$ (from k versus $\ln P$ data) and found it was approximately 1.4 for Barre granite and about 0.57 for pyroxene granulite. Data for Jones' coefficient B (equivalent to $\sqrt{2} b/e_0$ in Walsh formulation) is not available for volcanic tuff. For the calculations in this report, B was assumed to be unity.

Permeability versus stress relationships for MTS tuff would be valuable experimental data to obtain for future work. Both laboratory and field data would be useful. No studies have been completed on the correspondence of lab and field fracture permeability coefficients. Consequently, the necessary lab specimen size to obtain representative field values is not known (Witherspoon, 1981).

The effects of changes in both confining pressure (P_c) and the fluid pressure in the fracture (P_f) are usually combined to give an effective pressure (P_e). Traditionally P_e is defined as $P_c - P_f$ in soil mechanics, but Walsh (1981) points out the relationship $P_e = P_c - SP_f$ may be a more appropriate effective stress law for fractured media. This relationship is supported by test results of Kranz, et al (1978). The coefficient S relates to the pore volume and the compressibility of the surrounding rock. Appropriate values of S could be obtained from laboratory experiments relating k versus $\ln P_c$ for the material of interest. Because it was not possible to evaluate an effective pressure (P_e) in the

analysis, it was assumed P_c could be used in place of P_e as a rough approximation. The substitution implies an atmospheric fluid pore pressure.

From examination of the effective stress law and assuming $S < 1$, it is obvious that when P_c is much larger than P_f there should be little difference between P_e and P_c . The fact that Jones (1975) was successful in using confining pressure (P_c) in fitting data suggests the substitution is acceptable.

Postulated permeability-aperture product (ke) changes from the drill hole stress perturbation are plotted in Figure 4 for vertical-horizontal stress ratios (n) of 0.5, 1.0, 2.0. Examining the case where $n = 1.0$, the tangential joint intersection ($\nu = 1.0$) only reduced the permeability-aperture product (ke) a maximum of 31.5 percent ($x/a = 1.75$). The value of ke decreased 63.5 percent at this distance for $\nu = 0.0$. At the point of intersection with the drill hole, ke theoretically decreased 97.2 percent for $\nu = 0.0$ which suggests permeability changes could be substantial.

It is evident a tangential joint intersection minimizes the permeability changes for $n \leq 1$. This result follows directly from the cubic law and the plane strain, elastic analysis. But as indicated earlier, unusual stress behavior or cracking might occur in the region $0 < x/a < 1$ for a tangential intersection. It is also possible the joint would open. However, the increase in joint width and consequent permeability increase would be preferred. Entrance velocities would be lower. The experiment would thus simulate seepage conditions more realistically. A tangential intersection slightly increases permeability for $n > 1$ but similar arguments apply. Therefore, a tangential joint intersection is preferred in all cases.

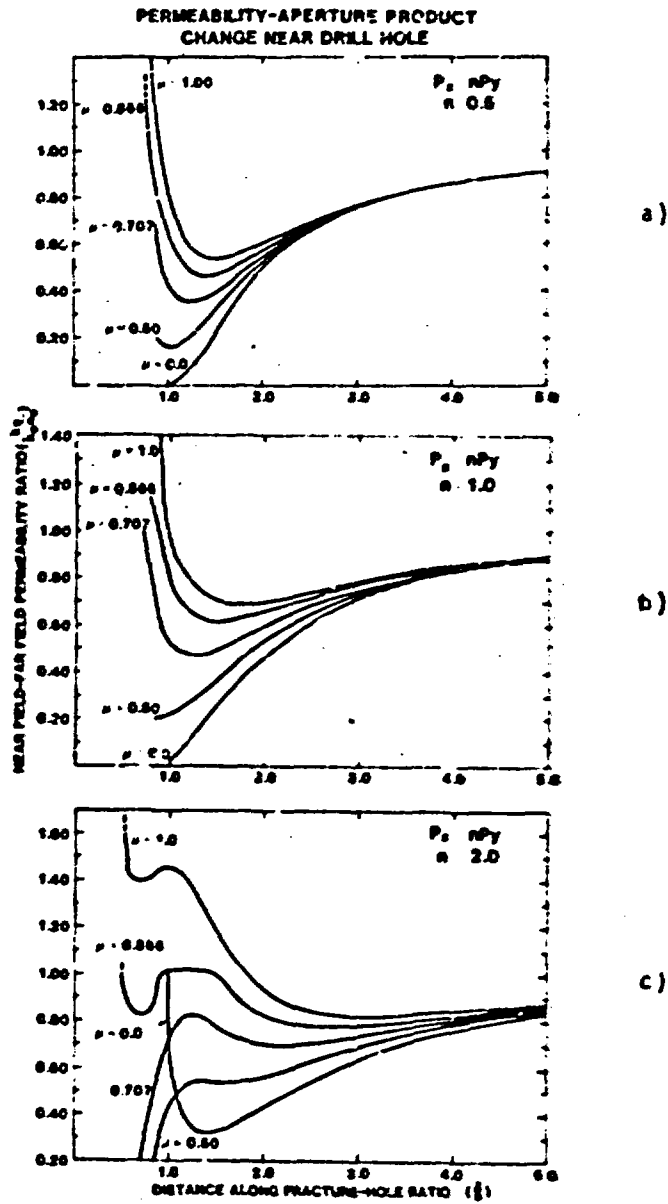


Figure 4. Postulated Permeability Changes Using Cubic Logarithmic Law, $P_x = nP_y$ a) $n = 0.5$ b) $n = 1.0$ c) $n = 2.0$.

CONCLUSIONS AND RECOMMENDATIONS

Based on the simplified analysis, a tangential intersection of the joint by the drill hole should be used to minimize disturbances of joint permeability in the field nuclide migration experiment. This assumes the instrumentation hole can be accurately placed along the joint.

The experiment will be difficult to perform and might benefit from a redesign to a perpendicular intersection of the joint by both the injection and collection holes. The radial flow experiment has two distinct advantages. First, the single fracture of interest does not have to be accurately traced. Brace (1978) and Witherspoon (1981) point out researchers have generally found large variations in individual joint behavior at distances greater than 1 m (3 ft). Second, the perpendicular intersection would eliminate normal stress concentrations along the joint. Laboratory experiments to date have avoided sheet-flow experiments (Iwai, 1976) in favor of the easily prepared and performed radial flow experiments.

A radial flow experiment can suffer from inherent hydraulic difficulties due to high inlet velocities with the potential to negate Darcy's law. Fortunately, velocities encountered at inlets for fractures are probably negligible (Iwai, 1976).

Although the perpendicular intersection would eliminate normal stress concentrations, small shear stresses could potentially develop during drilling. As a drill hole approached a joint, the rock mass above the joint would be free to relax while the lower portion would not. This situation would cause shear stresses along the joint. The shear stress could be diminished by drilling beyond the joint. Little data exist on the extent shear stress affects permeability. Conceivably dilatancy with a subsequent increase in permeability occurs if

the normal, in-situ stress is not large. Pratt, et al (1977) found that a 3 MPa (0.44 ksi) stress applied normal to a fractured 3 m (6 ft) block of granite halved the original permeability. It was necessary to apply 12 MPa (1.7 ksi) parallel to the joint to double the permeability. Thus, it can be tentatively assumed shear stress has less influence than normal stress on permeability.

REFERENCES

1. Bear, Jacob, 1972, Dynamics of Fluids in Porous Media, Elsevier, New York.
2. Byerlee, J. D., 1978, "Friction of Rocks," Pure and Applied Geophysics (PAGEOPH), Vol. 116, No. 4.
3. Erdal, B. R., et. al., 1981, "Nuclide Migration Field Experiments - Program Plan, Report No. LA-8787-MS, Los Alamos National Laboratory.
4. Gangi, A. F., 1978, "Variation of Whole and Fractured Porous Permeability with Confining Pressure," Int. J. Rock Mech. Min. Sci. and Geomech. Abstr., Vol. 15, pp 249-257.
5. Goodman, R. E., 1980, Introduction to Rock Mechanics, John Wiley and Sons, New York.
6. Iwai, Katsuhiko, 1976, "Fundamental Studies of Fluid Flow Through a Single Fracture," Ph. D. Thesis, Civil Eng., University of California, Berkeley.
7. Jones, F. O., 1975, "A Laboratory Study of the Effects of Confining Pressure on Fracture Flow and Storage Capacity in Carbonate Rocks, J. Petrol. Technol., Vol 21, pp 21-27.
8. Kranz, R. L., A. D. Frankel, T. Engelder, and C. H. Scholz, 1979, "The Permeability of Whole and Jointed Barre Granite," Int. J. Rock Mech. Min. Sci. and Geomech. Abstr., Vol. 16, pp 225-234.
9. Nelson, R. A., and J. Handin, 1977, "Experimental Study of Fracture Permeability in Porous Rock," Amer. Assoc. of Pet. Geol. Bull., Vol 61, No. 2., pp 227-236.
10. Walsh, J. B., 1981, "Effect of Pore Pressure and Confining Pressure on Rock Permeability," Seminar presented January 20, 1981 at Sandia National Laboratories.
11. Witherspoon, P. A., 1981, "Effect of Size on Fluid Movement in Rock Fractures," Geophysical Research Letters, Vol. 8, No. 7, pp 659-661.
12. Witherspoon, P. A., J. S. Y. Wang, K. Iwai, and J. E. Gale, 1980, "Validity of Cubic Law for Fluid Flow in a Deformable Rock Fracture," Water Resources Research, Vol. 16, No. 6, pp 1016-1024.

Distribution:
TIC-4700-R69 UC-70/305

W. Ballard, Director
Office of Waste Isolation
U.S. Dept. of Energy
Room B-207
Germantown, MD 20767

R. Stein, Acting Team Leader
Technology Team
U.S. Dept. of Energy
Room B-220
Germantown, MD 20767

J. O. Keff, Program Manager
National Waste Terminal
Storage Program Office
U.S. Dept. of Energy
505 King Avenue
Columbus, OH 43201

L. D. Ramspott
Technical Project Officer
Lawrence Livermore Nat. Lab.
University of California
P.O. Box 808
Mail Stop L-204
Livermore, CA 94550

A. R. Hahl, Site Manager
Westinghouse - AESD
P. O. Box 708
Mail Stop 703
Mercury, NV 89023

R. G. Goranson
U.S. Dept. of Energy
Richland Operations Office
P. O. Box 550
Richland, WA 99352

D. F. Miller, Director
Office of Public Affairs
U.S. Dept. of Energy
P. O. Box 14100
Las Vegas, NV 89114

B. W. Church, Director
Health Physics Division
P. O. Box 14100
Las Vegas, NV 89114

G. L. Dixon
Technical Project Officer
U.S. Geological Survey
P. O. Box 25046
Mail Stop 954
Federal Center
Denver, CO 80225

W. E. Wilson
U.S. Geological Survey
P.O. Box 25046
Mail Stop 416
Denver, CO 80225

W. S. Twenhofel
820 Estes Street
Lakewood, CO 80215

B. R. Erdal
Tech. Project Officer
Los Alamos Nat. Lab.
University of California
P. O. Box 1663
Mail Stop 514
Los Alamos, NM 87545

C. R. Cooley
Deputy Director
U. S. Dept. of Energy
Room B-214
Germantown, MD 20767

R. Deju
Rockwell International
Atomic Intl. Div.
Rockwell Hanford Operations
Richland, WA 99352

R. M. Nelson, Director (3)
Waste Management Proj. Office
U.S. Dept. of Energy
P. O. Box 14100
Las Vegas, NV 89114

R. H. Marks
U. S. Dept. of Energy
CP-1, M/S 210
P. O. Box 14100
Las Vegas, NV 89114

R. R. Loux (7)
U.S. Dept. of Energy
P. O. Box 14100
Las Vegas, NV 89114

K. Street, Jr.
LLNL
Univ. of California
Mail Stop L-209
P. O. Box 808
Livermore, CA 94550

W. A. Carbiener
Battelle
Office of NWS Integration
505 King Avenue
Columbus, OH 43201

S. Goldsmith
Battelle
Office of Nuc. Waste Isolation
505 King Avenue
Columbus, OH 43201

R. M. Hill
State Planning Coordinator
Governor's Office of
Planning Coordination
Capitol Complex
Carson City, NV 89023

H. D. Cunningham
Reynolds Elec. Engr. Co. Inc.
Mail Stop 555
P. O. Box 14400
Las Vegas, NV 89114

J. A. Cross
Fenix Scisson, Inc.
P. O. Box 15408
Las Vegas, NV 89114

A. J. Rothman (2)
LLNL, MS L-204
University of California
P. O. Box 808
Livermore, CA 94550

A. E. Gurrola
Holmes Narver, Inc.
P. O. Box 14340
Las Vegas, NV 89114

D. C. Hoffman
LANL
Mail Stop 760
P. O. Box 1663
Los Alamos, NM 87545

N. E. Carter
Battelle
Office of Nuc. Waste
Isolation
505 King Avenue
Columbus, OH 43201

ONWI Library (5)
Battelle
Of. of Nuc. Waste Isolation
505 King Avenue
Columbus, OH 43201

N. A. Clark
Dept. of Energy
State of Nevada
Capitol Complex
Carson City, NV 89710

J. P. Colton
International Atomic Energy
Agency
Div. of Nuc. Power Reactors
Wagarmstrasse 5
P. O. Box 100, A-1400
Vienna, Austria

A. M. Friedman
Argonne Nat. Laboratories
9700 S. Cass Avenue
Argonne, IL 60439

1417 F. W. Muller
4760 R. W. Lynch
4761 L. W. Scully
4762 L. D. Tyler
4763 J. R. Tillerson
4763 B. S. Langkopt
4763 A. R. Lappin
4763 R. M. Zimmerman
4763 R. Shaw
4764 R. C. Lincoln
4764 A. E. Stephenson
5500 O. E. Jones
5510 D. B. Hayes
5511 J. W. Nunziato
5511 D. K. Gartling
5520 T. B. Lane
5521 R. D. Krieg
5521 R. D. Thomas
5522 T. G. Priddy
5522 R. P. Rechar (5)
5522 K. W. Schuler (5)
5530 W. Herrmann
5531 M. L. Blanford
5532 B. M. Butcher
5532 W. A. Olsson
5541 W. C. Luth
8266 F. A. Aas
3141 L. J. Erickson
3151 W. L. Garner
For: DOE/TIC (Unlimited Release) (3)
3154-3 C. H. Dalin
For DOE/TIC (25)